

Reflectivity Is All You Need!: Advancing LiDAR Semantic Segmentation

Kasi Viswanath, Peng Jiang and Srikanth Saripalli

Abstract—LiDAR semantic segmentation frameworks predominantly leverage geometry-based features to differentiate objects within a scan. While these methods excel in scenarios with clear boundaries and distinct shapes, their performance declines in environments where boundaries are blurred, particularly in off-road contexts. To address this, recent strides in 3D segmentation algorithms have focused on harnessing raw LiDAR intensity measurements to improve prediction accuracy. Despite these efforts, current learning-based models struggle to correlate the intricate connections between raw intensity and factors such as distance, incidence angle, material reflectivity, and atmospheric conditions. Building upon our prior work[1], this paper delves into the advantages of employing calibrated intensity (also referred to as reflectivity) within learning-based LiDAR semantic segmentation frameworks. We initially establish that incorporating reflectivity as an input enhances the existing LiDAR semantic segmentation model. Furthermore, we present findings that enable the model to learn to calibrate intensity can boost its performance. Through extensive experimentation on the off-road dataset Rellis-3D, we demonstrate notable improvements. Specifically, converting intensity to reflectivity results in a 4% increase in mean Intersection over Union (mIoU) when compared to using raw intensity in Off-road scenarios. Additionally, we also investigate the possible benefits of using calibrated intensity in semantic segmentation in urban environments (SemanticKITTI) and cross-sensor domain adaptation. [Github repository](#)

I. INTRODUCTION

LiDAR (Light Detection and Ranging) semantic segmentation has become a crucial technology in autonomous driving and robotics, providing a detailed three-dimensional perspective of the surrounding environment. This process involves categorizing each point in a LiDAR point cloud into distinct classes, such as vehicles, pedestrians, trees, and buildings, enabling machines to perceive and interact with their environments. In autonomous vehicles, LiDAR semantic segmentation is essential for obstacle detection, navigation, and path planning, facilitating informed decisions in complex and dynamic contexts. The integration of this technology ensures autonomous systems can operate safely and efficiently in human-centric environments, driving the evolution of intelligent systems in our increasingly automated society.

However, traditional learning based LiDAR semantic segmentation models have primarily focused on the geometric characteristics of objects. For example, deep learning models like SalsaNext [2] [3] utilize encoder-decoder architectures to analyze raster laser scan images, where four out of five channels convey geometry information ($range, x, y, z$).

Kasi Viswanath, Peng Jiang and Srikanth Saripalli are with the Department of Mechanical Engineering, Texas A&M University, College Station, TX-77843 kasiv,maskjp,ssaripalli@tamu.edu

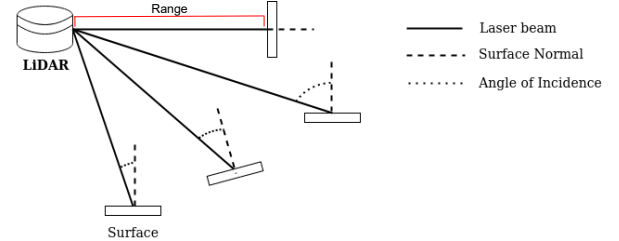


Fig. 1. Interaction of laser beam with the surface at a different angle of incidence.

Meanwhile, Cylinder3D [4] employs 3D sparse convolution operations to probe the laser scan’s 3D topology through cylindrical partitioning, leveraging 3D geometric characteristics to extract semantic features. Although these approaches are effective in urban settings with distinct edges and shapes, they may face challenges in more complex, unstructured off-road environments. Notably, both models incorporate the LiDAR return’s intensity as an auxiliary input to enhance learning. However, these intensity values, which are influenced by factors such as range, incidence angle, and surface features, are not well calibrated, leading to distortion of meaningful information. Calibrating intensity values in LiDAR data, by eliminating dependencies on range and angle of incidence and focusing solely on reflectivity, demonstrates an object’s ability to reflect radiation. When this calibration is done accurately, it can notably enhance the visual quality of projected LiDAR data, providing finer-grained and more insightful details (see Fig. 4). It is noteworthy that in this paper, *calibrated intensity* and *reflectivity* are used interchangeably to refer to a parameter distinct from raw intensity.

Research on LiDAR intensity has been predominantly undertaken in the geospatial area, focusing on segmenting aerial LiDAR scans to discern distinct features like vegetation, buildings, and roads [5] [6]. In terrestrial laser scanning, calibrated intensity data proves crucial for applications such as urban roadway lane detection and vegetation monitoring [7] [8]. The calibration of intensity for improved reflectivity measurement has thus become a key research objective aimed at enhancing the interpretation of sensor data. Notably, research has introduced innovative approaches for data collection and calibration; [9] proposed a novel design for collecting sample data in controlled environments to estimate parameters for a customized range-intensity equation for terrestrial laser scanners. [10] outlined a new empirical calibration method for laser scanner intensity, utilizing brightness targets and a calibrated reference panel in both laboratory and field conditions. However, these studies have largely

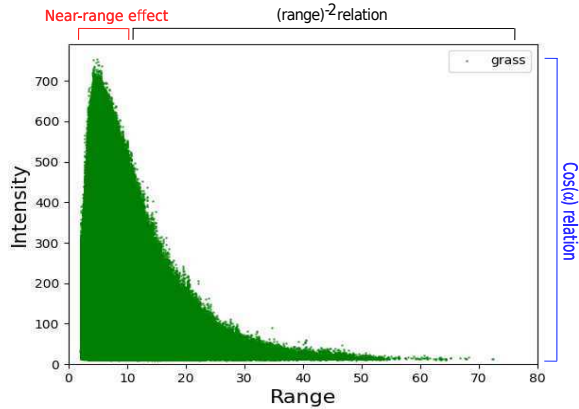


Fig. 2. Comparison of raw intensity versus range for the grass class. The figure demonstrates how intensity varies with range and angle of incidence. It highlights the relationship between angle of incidence and intensity, indicating that the greatest intensity at each range is achieved when α nears 0, while the lowest intensity occurs when α is approximately $\pi/2$.

concentrated on terrestrial laser scanners, with mobile LiDAR systems, extensively used in autonomous vehicles and robotics, receiving less attention. Datasets widely recognized in the field, such as SemanticKITTI[11] or RELLIS3D[12], often feature uncalibrated LiDAR data. To address this gap, recent efforts have been made to explore the calibrated intensity of mobile LiDAR. [1] introduced a hybrid method for calibrating intensity values based on range and incidence angle, demonstrating its utility for object segmentation in off-road environments through traditional clustering methods. Nevertheless, this exploration primarily assessed the advantages of calibrated intensity with conventional clustering algorithms and a limited array of object classes. A significant limitation of traditional methods is their struggle with high-dimensional data, which can result in inaccuracies when clustering complex multi-object scenes.

Advancing from the foundation, this paper explores the combination of LiDAR intensity data with geometric details to augment existing deep-learning models for broader class categorization. This research introduces a novel approach that fuses reflectivity data with neural network models to refine segmentation further. By leveraging the detailed insights offered by reflectivity values, we aim to establish a more robust framework for LiDAR semantic segmentation capable of addressing the intricacies of off-road terrains. Our findings reveal that incorporating reflectivity data considerably improves the performance of existing LiDAR semantic segmentation models, indicating a promising pathway for future advancements in the field. The primary contributions of this work are:

- Development of a data-driven approach for calibrating near-range intensity measurements.
- Investigation into the utility of LiDAR reflectivity as an input feature for enhancing current state-of-the-art segmentation models.
- Incorporation of reflectivity learning through SalsaNext model and shows a boost in segmentation performance.
- Proposal of a unified LiDAR intensity representation

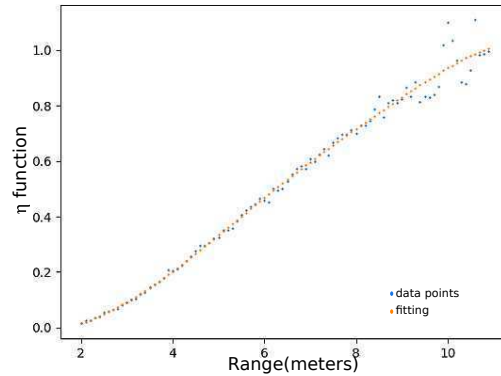


Fig. 3. Estimated $\eta(R)$ function for Ouster-64.

to enable cross-sensor calibration, thereby improving domain adaptation capabilities.

II. METHOD

A. Revisit LiDAR Intensity Calibration

1) *LiDAR Intensity Equation and Nearrange Effect*: The intensity of a LiDAR signal is influenced by the distance to the target (range) and the angle at which the signal strikes the target (angle of incidence) (see Figure 1). The relationship between these factors is encapsulated by the LiDAR intensity equation [13]:

$$I(R, \alpha, \rho) \propto P_r(R, \alpha, \rho) = \eta(R) \frac{I_e \rho \text{Cos}(\alpha)}{R^2} \quad (1)$$

where I_e denotes the laser's emission power, R signifies the distance to the surface, α represents angle of incidence, and ρ is the parameter indicating the target's reflectivity.

Due to lens defocusing in LiDAR sensors, as detailed by Biavati et.al.[14], a near-range effect, denoted as $\eta(R)$, significantly impacts the intensity data at closer ranges ($R_n < 12$ meters). This phenomenon causes Equation 1 to be inapplicable within these proximities. We adopt the modeling approach for the near-range effect as outlined in [9], which is described as follows:

$$\eta(R) = 1 - \exp\left\{\frac{-2r_d^2(R+d)^2}{D^2 S^2}\right\} \quad (2)$$

with r_d denotes the radius of the laser detector, d represents the offset between the measured range and object distance, D is the diameter of the lens, and S signifies focal length, respectively. These parameters can be estimated through controlled experiments [9], which is laborious. In this paper propose a data driven approach to estimate the near-range parameter $\eta(R)$ through semantically annotated datasets.

2) *Near-range effect parameter estimation*: For LiDAR points situated beyond the influence of the near-range effect, the intensity is dependent solely by the reflectivity coefficient, the range, and the angle of incidence. The reflectivity coefficients for these extended ranges are determined by calibrating the intensity according to the following equation:

$$I_c(\rho) \approx \frac{I_c(R, \alpha, \rho) \times R^2}{\text{cos}(\alpha)}; R > R_n \quad (3)$$

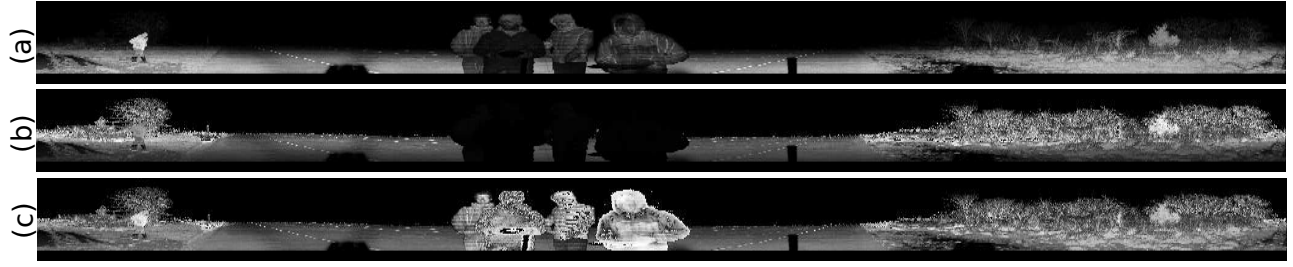


Fig. 4. Spherical projection of a) Raw intensity data b) Calibrated intensity for Range and angle of incidence(α) c) Calibrated intensity for near-range (η), range and angle of incidence(α).

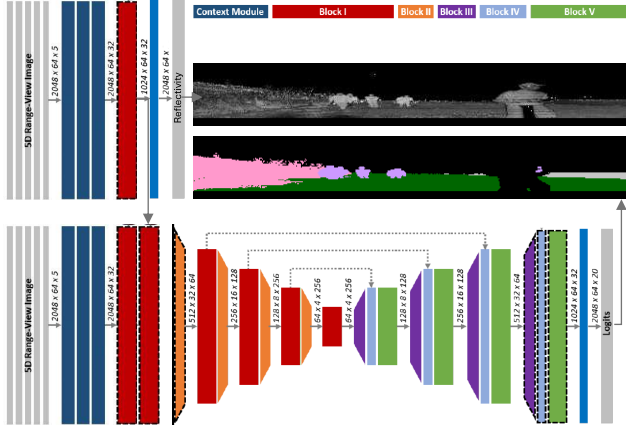


Fig. 5. Learning Reflectivity model (Picture modify from SalsaNext[2])

where R_n represents the distance within the influence of near-range effect. Utilizing the annotated labels, the reflectivity coefficients are clustered, yielding a centroid $I_c(\rho)$ for each class. As the reflectivity coefficients remain constant throughout the entire range, $\eta(R)$ function for each class can be derived as follows:

$$\eta(R) = \frac{I_c(R, \alpha, \rho) \times R^2}{I_c(\rho) \times \cos(\alpha)} \quad (4)$$

This analysis reveals that the $\eta(R)$ function, indicative of the sensor's characteristics, remains consistent across different objects or classes. The $\eta(R)$ function derived for the Ouster sensor within the Rellis-3D dataset is illustrated in Figure 3.

3) *Calibrating Intensity*: With $\eta(R)$, range and angle of incidence known, the raw intensity $I(R, \alpha, \rho)$ of a point cloud can be calibrated to provide reflectivity coefficients $I(\rho)$ using the following equation:

$$I(\rho) = \frac{I(R, \alpha, \rho) \times R^2}{\cos(\alpha) \times \eta(R)} \quad (5)$$

An example of intensity before and after calibration is shown in Figure 4.

4) *Cross-Sensor Calibration*: Different LiDAR sensors output intensity data in varying formats. For instance, Velodyne sensors undergo an in-house calibration process for range and power, which is claimed to improve the capabilities of object identification. Given that intensity is a critical feature for semantic segmentation, a model trained on data from one sensor suite often underperforms when applied to data

from another sensor, even within identical scenes[15]. This discrepancy poses significant challenges for the robustness of LiDAR segmentation frameworks and impedes effective cross-domain adaptation.

In our previous research [1], we introduced a pre-processing technique designed to transform Velodyne data into the Ouster format. This transformation is significant because the Ouster format retains the raw form of the LiDAR equation, as illustrated in Figure 2. The conversion employs a fitting function that is consistently applied across all object classes.

B. Leveraging Reflectivity in Deep Learning Models

II-B.2 To demonstrate the advantages of incorporating reflectivity, we conducted experiments and made modifications to SalsaNext [2]. Although not the state-of-the-art (SOTA) model on the SemanticKitti benchmark, SalsaNext excels in off-road scenarios, outperforming the SOTA models on SemanticKITTI. SalsaNext features an encoder-decoder architecture, with the encoder comprising a stack of residual dilated convolutions, and the decoder combining features upsampled from the residual blocks with a pixel-shuffle layer. It employs leaky ReLU activation followed by batch normalization to address covariate shift. The architecture is identical to the model depicted in Figure 5, except it lacks the reflectivity output head.

1) *Incorporating Reflectivity as an Input*: The original model processes inputs as five spherical projections [16] of the LiDAR scan— x, y, z , range, and intensity [$h \times w \times 5$], as illustrated in Fig. 4. It maintains neighborhood features and emphasizes the intensity parameter, effectively treating it as a grayscale image. To substantiate our hypothesis, we replaced the intensity with calibrated intensity, and we present our findings in Section III-B.

2) *Learning to Predict Reflectivity*: Calibrating intensity for LiDAR data involves calculating the surface normal and range for each point, in addition to knowing the LiDAR calibration parameters. This process can be cumbersome during inference for LiDAR semantic segmentation. To address this issue, we introduce a modified version of the SalsaNext model equipped with an auxiliary head designed to predict calibrated intensity directly. This adaptation allows the model to use the standard inputs (x, y, z coordinates, range, and intensity) without the need for further calibration steps for intensity. In our preliminary experiments, we explored two

Dataset	Config	Grass	Tree	Pole	Vehicle	Log	Person	Fence	Bush	Concrete	Barrier	Puddle	Mud	Rubble	mIoU
Rellis-3D	rxysi	35.1	49.6	56.1	23.8	14.5	62.8	0.6	30.2	50.0	80.1	20.4	10.7	66.6	38.4
	rxyzn	37.6	55.7	52.3	21.4	10.3	76.0	1.4	33.9	74.5	81.3	25.0	13.7	67.7	42.4
	rxyzirn	36.2	55.8	51.0	20.3	9.9	82.7	2.7	34.0	60.1	79.1	22.6	12.9	68.9	41.2
	rxysi_gau	36.0	58.4	52.5	22.2	12.6	82.6	3.2	35.7	59.9	80.9	24.2	12.5	63.8	41.9
Source	Target	Grass	Tree	Pole	Vehicle	Log	Person	Fence	Bush	Concrete	Barrier	Puddle	Mud	Rubble	mIoU
OS rxysi	VLP rxysi	19.6	40.3	0.1	0.0	0.0	2.1	0.0	33.9	1.7	0.0	0.0	0.3	0.2	7.5
OS rxyzn	VLP rxyzn	30.3	38.3	1.1	4.8	0.2	34.1	0.9	35.4	27.3	3.8	1.6	0.9	0.3	13.8

TABLE I

mIoU OF EXPERIMENT RESULTS ON RELLIS-3D WITH DIFFERENT INPUT CONFIGURATION AND CROSS-SENSOR ADAPTATION

Dataset	Config	Car	Bicycle	Motorcycle	Truck	Other-vehicle	Person	Bicyclist	Motorcyclist	Road	Parking	Sidewalk	Other-ground	Building	Fence	Vegetation	Trunk	Terrain	Pole	Traffic Sign	mIoU
Semantic-kitti	rxysi	90.9	37.1	51.8	83.4	43.0	68.7	82	0.1	77.4	44.8	60.1	6.0	73.2	45.9	46.1	64.1	47.9	56.3	46.8	54.0
	rxyzn	92.4	44.8	52.5	71.4	46.9	69.5	84.6	0	78.6	44.4	59.6	0.3	73.6	49.9	45.5	64.7	48.0	58.1	45.6	54.2
	rxyzirn	92.0	41.3	50.4	75.3	48.5	70.5	83.0	0	77.2	43.4	59.1	0.2	74.9	49.8	51.6	66.0	54.0	57.0	47.0	54.8
	rxysi_gau	91.9	44.4	43.6	58.6	44.7	70.2	84.8	0.0	79.7	46.5	60.5	10.0	73.4	48.8	45.5	64.7	48.3	58.6	45.3	53.7

TABLE II

mIoU OF EXPERIMENT RESULTS ON SEMANTICKITTI VALIDATION SET WITH DIFFERENT INPUT CONFIGURATION

approaches: late prediction and early prediction. The late prediction approach involves adding an extra convolution layer to the end of the SalsaNext model, specifically for predicting calibrated intensity. Unfortunately, this method was not successful and adversely affected the performance of the primary semantic segmentation task. Conversely, in the early prediction approach, we integrated three convolution layers early in the model to focus on predicting calibrated intensity. Instead of directly using the predicted reflectivity, we took the final feature outputs from this auxiliary head and merged them with the intermediate features from the main SalsaNext model. This approach aims to leverage the calibrated intensity information more effectively within the segmentation process.

The factors influencing intensity include range, surface normal, surface color, surface material, humidity, among others. Furthermore, we utilize calibrated intensity as the ground truth for learning; however, these measurements are not always accurate. To address variability across classes, we model the calibrated intensity for each class using a Gaussian distribution. Rather than employing traditional loss functions such as L1 loss or mean square loss, we opt for the Gaussian negative log likelihood loss as follows:

$$L = \sum_{c=1}^{classes} \frac{1}{2} \left(\log(\text{var}(I_e^c)) + \frac{(I^c - I_e^c)^2}{\text{var}(I_e^c)} \right) \quad (6)$$

where I^c represents the input intensity, and I_e^c denotes the calibrated intensity for class c .

III. EXPERIMENTAL RESULTS

A. Experiment Setup

To evaluate the impact of reflectivity on the effectiveness of LiDAR semantic segmentation, we conducted multiple experiments. First, we experiment with how the model will be benefited by simply using reflectivity as input. We first trained the SalsaNext model under its original settings,

utilizing inputs comprising x, y, z coordinates, $range$, and intensity ($xyzri$). Then, we replace the intensity with two distinct types of reflectivity inputs: 1) Calibrated intensity without near-range correction and 2) Calibrated intensity with near-range correction. The input configurations were selected as:

- 1) range, x, y, z , intensity ($rxysi$);
- 2) range, x, y, z , near-range calibrated reflectivity ($rxyzn$);
- 3) range, x, y, z , reflectivity, near-range calibrated reflectivity ($rxyzirn$).

In our fourth experimental setup, we assess the performance of the model and loss function introduced in Section II-B.2, denoting these trials as $rxysi_gau$. To maintain consistency across all experiments, key model parameters—including learning rate, weight decay, and batch size—were held constant, with the exception of the loss function specifically for the $rxysi_gau$ configuration. This approach ensures that any variations in performance can be attributed directly to the changes in the model and loss function rather than external variables.

B. Quantitative Results

1) *Off-Road Environment*: Our primary focus is on off-road domains; consequently, we prioritize conducting experiments in off-road environments. For this purpose, we selected the Rellis-3D dataset, which contains semantically annotated LiDAR scans from the Ouster-OS1 64-channel scanner, specifically tailored for off-road scenarios. The performance outcomes are detailed in Table I. When using the $rxyzn$ input configuration, SalsaNext achieved a mean Intersection over Union (mIoU) of 42.4%, marking a 4% improvement over the model trained with the $rxysi$ input. Furthermore, training SalsaNext with the $rxyzirn$ input configuration resulted in a 3% increase in mIoU, underscoring the advantage of incorporating reflectivity for enhanced feature learnability over intensity alone. In another noteworthy result, SalsaNext

achieved the second highest mIoU of 41.9% in a fourth setting, illustrating the model’s capability to internalize the calibration process, thereby boosting performance. Notably, in this configuration, the model efficiently utilizes only the raw point cloud data with intensity for inference, showcasing its practical adaptability.

2) *Cross-sensor*: Rellis-3D also features annotated scans from the Velodyne VLP-32 LiDAR for the same environments. It is important to note that Velodyne LiDAR systems output intensity values as pre-calibrated 8-bit integers. To assess the effectiveness of cross-sensor applicability, we conducted tests where a SalsaNext model trained on the Ouster *rxzyi* (intensity) configuration was evaluated on Velodyne *rxzyi* data, and a model trained on Ouster *rxyzn* (near-range calibrated reflectivity) was tested on Velodyne *rxyzn*. The comparative results, presented in Table I, reveal that the model trained on Ouster *rxyzn* outperformed the one trained on Ouster *rxzyi*, showing a significant 6% increase in mean Intersection over Union (mIoU) and leading in 12 out of 13 categories.

3) *Urban Environment*: For urban environment testing, we utilize the SemanticKITTI dataset, a multi-modal dataset designed for urban environments, which features annotated LiDAR scans from the Velodyne HDL-64E. The performance on SemanticKITTI is detailed in Table II, highlighting the efficacy of different input configurations. The configuration denoted as *rxzyirn* achieved the highest mean Intersection over Union (mIoU) at 54.8%, followed closely by *rxyzn* at 54.2%, and the baseline configuration *rxzyi*, which also demonstrated competitive performance, achieving a 54.0% mIoU.

C. Qualitative Results

Qualitative analysis was performed on Rellis-3D, with SalsaNext input configurations *rxzyi* and *rxyzn* as shown in Figure 6. Figure 6 compares predictions with ground truth represented in spherical projection and camera projection of segmented object points. (Note: SalsaNext doesn’t use images for training, and the figure is only for visualization purposes.) The figure shows that the predictions from *rxyzn* provide better boundaries for puddles and dirt than predictions from *rxzyi* and even ground truth. Moreover, the ground truth labels dirt surrounding the puddle region as a puddle, and many more instances of incorrect labeling can be found in the Rellis-3D dataset. This could be attributed to the overall low performance of SalsaNext across all configurations.

Qualitative analysis of the SemanticKITTI dataset revealed that models using reflectivity and those employing intensity produce similar predictions. This observation underscores the significant contrast or variation in intensity values observed within urban scenes, suggesting that intensity alone can suffice for the effective segmentation of various objects.

D. Runtime Evaluation

Given the critical importance of inference speed in the field of autonomous driving, we have meticulously optimized

the calibration and prediction processes to facilitate real-time inference. Our framework, which includes LiDAR intensity calibration for near-range, range, and angle of incidence, coupled with SalsaNext prediction, achieves a processing speed of 20 Hz (approximately 50 ms) on an Nvidia RTX 4070 GPU. Considering that LiDAR sensors commonly publish point cloud data at 10 Hz, our methodology ensures real-time inference of scans while maintaining accuracy comparable to other cutting-edge segmentation frameworks.

IV. INFERENCE

The experiments conducted on the Rellis-3D and SemanticKITTI datasets indicate that utilizing reflectivity rather than intensity yields improved segmentation results in both off-road and on-road contexts. The notable enhancement in accuracy observed in off-road scenes can be attributed to the reflectivity parameter’s ability to distinguish between classes. This is particularly crucial as objects within the same class maintain consistent color and texture, while variations exist across different classes. Given the unstructured nature of off-road environments and the presence of loose boundaries, relying solely on geometry-based features resulted in lower performance.

In urban settings, where boundaries are clearly delineated across scenes, geometric features play a more significant role in learning compared to reflectivity/intensity parameters. Additionally, variations in intensity values between objects, such as different intensity values for cars based on surface color and texture, can also impact segmentation results. These factors may contribute to the limited improvement observed when using reflectivity in SemanticKITTI experiments. Nevertheless, it is noteworthy that incorporating reflectivity consistently led to enhanced segmentation results compared to intensity across all experiments.

After conducting cross-sensor experiments on the Rellis-3D dataset, it is clear that transferring a model from one sensor to another, even within the same scene, produces unsatisfactory outcomes. Although LiDAR intensity calibration has been effective in enhancing results, other factors such as the number of rings, ray pattern, and field of view have notable impacts on cross-domain capability.

V. DISCUSSION AND CONCLUSION

In our study, we have showcased the promise of leveraging calibrated LiDAR intensity to enhance semantic segmentation. By incorporating reflectivity, Salsanext yielded a 4% increase in mIoU score on Rellis-3D and exhibited superior boundary predictions compared to intensity alone. While calibration ensures accuracy, adverse weather conditions like rain, snow, and fog can disrupt LiDAR performance, resulting in inaccurate point clouds due to particle interference. Therefore, future efforts will focus on resilient sensors like radar, which can offer precise data even in challenging weather conditions. Based on these findings, we advocate for the robotics community to transition from intensity to reflectivity and to pursue the development of specialized

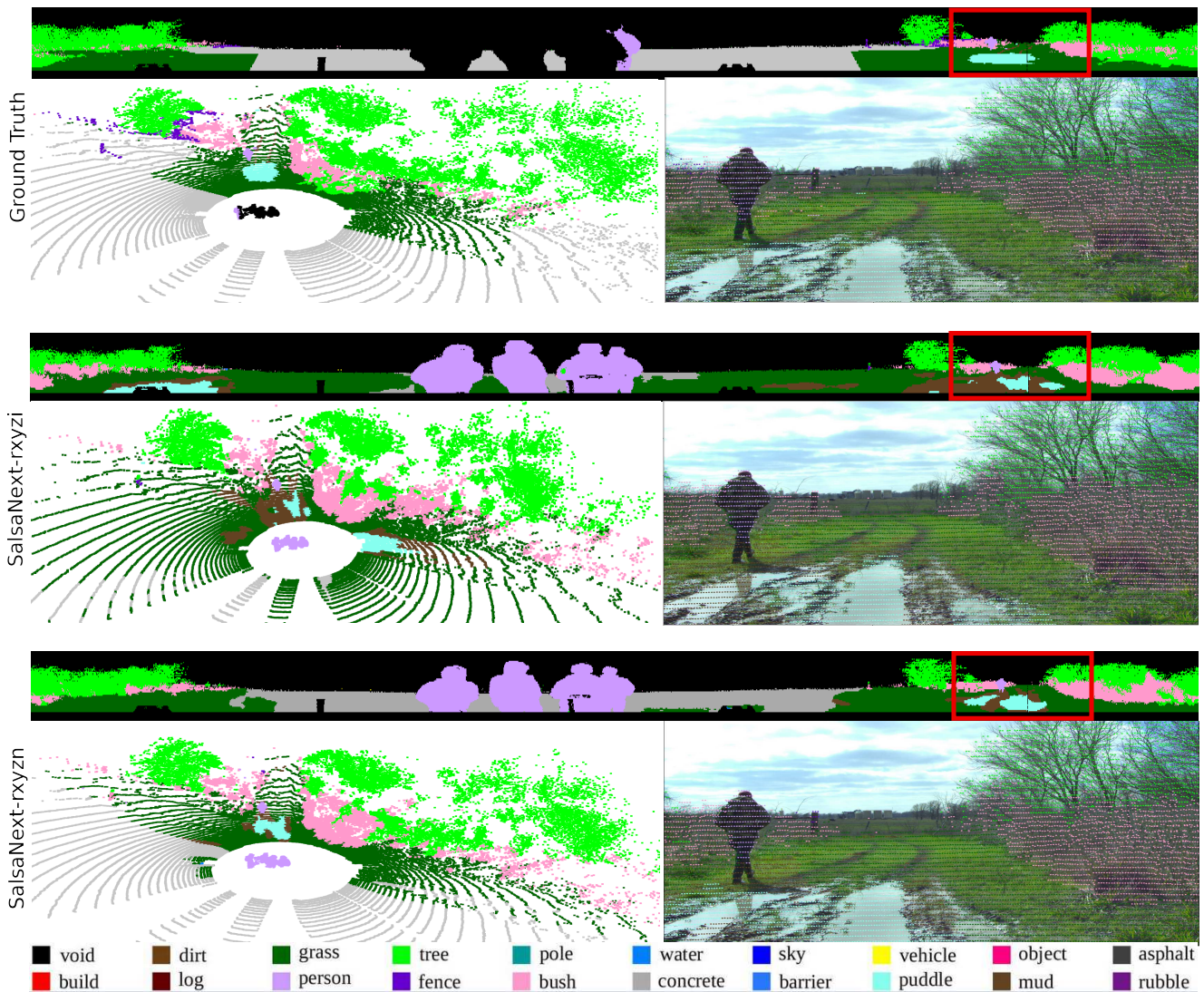


Fig. 6. Sample qualitative results from a test set of Rellis-3D. The image shows a spherical projection of point cloud labels for ground truth, Salsanext-*rxyz* and Salsanext-*rxyzn* predictions, along with labeled point cloud projection and camera projections.

segmentation models that capitalize on the reflectivity parameter.

REFERENCES

- [1] K. Viswanath, P. Jiang, S. PB, and S. Saripalli, "Off-road lidar intensity based semantic segmentation," *arXiv preprint arXiv:2401.01439*, 2024.
- [2] T. Cortinhal, G. Tzelepis, and E. Erdal Aksoy, "Salsanext: Fast, uncertainty-aware semantic segmentation of lidar point clouds," in *Advances in Visual Computing*, G. Bebis, Z. Yin, E. Kim, J. Bender, K. Subr, B. C. Kwon, J. Zhao, D. Kalkofen, and G. Baciú, Eds. Cham: Springer International Publishing, 2020, pp. 207–222.
- [3] E. E. Aksoy, S. Baci, and S. Cavdar, "Salsanet: Fast road and vehicle segmentation in lidar point clouds for autonomous driving," in *2020 IEEE Intelligent Vehicles Symposium (IV)*, 2020, pp. 926–932.
- [4] X. Zhu, H. Zhou, T. Wang, F. Hong, Y. Ma, W. Li, H. Li, and D. Lin, "Cylindrical and asymmetrical 3d convolution networks for lidar segmentation," *arXiv preprint arXiv:2011.10033*, 2020.
- [5] A. Novo, N. Fariñas-Álvarez, J. Martínez-Sánchez, H. González-Jorge, and H. Lorenzo, "Automatic processing of aerial lidar data to detect vegetation continuity in the surroundings of roads," *Remote Sensing*, vol. 12, no. 10, 2020. [Online]. Available: <https://www.mdpi.com/2072-4292/12/10/1677>
- [6] W. Luo, S. Gan, X. Yuan, S. Gao, R. Bi, and L. Hu, "Test and analysis of vegetation coverage in open-pit phosphate mining area around dianchi lake using uav-vdvi," *Sensors*, vol. 22, no. 17, 2022. [Online]. Available: <https://www.mdpi.com/1424-8220/22/17/6388>
- [7] J. Jung and S.-H. Bae, "Real-time road lane detection in urban areas using lidar data," *Electronics*, vol. 7, no. 11, 2018. [Online]. Available: <https://www.mdpi.com/2079-9292/7/11/276>
- [8] K. Tan, W. Zhang, Z. Dong, X. Cheng, and X. Cheng, "Leaf and wood separation for individual trees using the intensity and density data of terrestrial laser scanners," *IEEE Transactions on Geoscience and Remote Sensing*, vol. 59, no. 8, pp. 7038–7050, 2021.
- [9] W. Fang, X. Huang, F. Zhang, and D. Li, "Intensity correction of terrestrial laser scanning data by estimating laser transmission function," *IEEE Transactions on Geoscience and Remote Sensing*, vol. 53, no. 2, pp. 942–951, 2015.
- [10] S. Kaasalainen, A. Kukko, T. Lindroos, P. Litkey, H. Kaartinen, J. Hyypä, and E. Ahokas, "Brightness measurements and calibration with airborne and terrestrial laser scanners," *IEEE Transactions on Geoscience and Remote Sensing*, vol. 46, no. 2, pp. 528–534, 2008.
- [11] J. Behley, M. Garbade, A. Milioto, J. Quenzel, S. Behnke, C. Stachniss, and J. Gall, "SemanticKITTI: A Dataset for Semantic Scene Understanding of LiDAR Sequences," in *Proc. of the IEEE/CVF International Conf. on Computer Vision (ICCV)*, 2019.
- [12] P. Jiang, P. Osteen, M. Wigness, and S. Saripalli, "Rellis-3d dataset: Data, benchmarks and analysis," in *2021 IEEE International Confer-*

- ence on Robotics and Automation (ICRA), 2021, pp. 1110–1116.
- [13] A. V. Jelalian, “Laser radar systems,” in *EASCON 1980: Electronics and Aerospace Systems Conference*, Jan. 1980, pp. 546–554.
- [14] G. Biavati, G. D. Donfrancesco, F. Cairo, and D. G. Feist, “Correction scheme for close-range lidar returns,” *Appl. Opt.*, vol. 50, no. 30, pp. 5872–5882, Oct 2011. [Online]. Available: <https://opg.optica.org/ao/abstract.cfm?URI=ao-50-30-5872>
- [15] L. Wang, D. Li, Y. Zhu, L. Tian, and Y. Shan, “Cross-dataset collaborative learning for semantic segmentation,” *CoRR*, vol. abs/2103.11351, 2021. [Online]. Available: <https://arxiv.org/abs/2103.11351>
- [16] A. Milioto, I. Vizzo, J. Behley, and C. Stachniss, “Rangenet ++: Fast and accurate lidar semantic segmentation,” in *2019 IEEE/RSJ International Conference on Intelligent Robots and Systems (IROS)*, 2019, pp. 4213–4220.